

# Effect of the oxygen isoelectronic substitution in $\text{Cu}_2\text{ZnSnS}_4$ and its photovoltaic application

C. Tablero

## ABSTRACT

The optoelectronic properties of  $\text{Cu}_2\text{ZnSnS}_4$  and environmental considerations have attracted significant interest for photovoltaics. Using first-principles, we analyze the possible improvement of this material as a photovoltaic absorber via the isoelectronic substitution of S with O atoms. The evolution of the acceptor level is analyzed with respect to the atomic position of the nearest neighbors of the O atom. We estimate the maximum efficiency of this compound when used as a light absorber. The presence of the sub-band gap level below the conduction band could increase the solar-energy conversion with respect to the host.

## 1. Introduction

The  $\text{Cu}_2\text{ZnSnS}_4$  (CZTS) semiconductor has attracted a significant interest due to it having similar properties to chalcopyrites  $\text{Cu}(\text{In}, \text{Ga})(\text{S}, \text{Se})_2$ , a candidate already commercialized for large-scale photovoltaic modules, based thin-film technology, with efficiencies above 10%. In these materials, In and/or Ga are replaced with earth-abundant Zn and Sn metals. Higher sulfur compositions yield band gap values corresponding to the theoretical maximum for single-band gap solar energy conversion ( $\sim 40\%$ ), while selenium introduction decreases the band gap. Band gap values between 1.4 eV [1] and 1.6 eV [2] have been reported for CZTS. It is assumed that this is due to deviations from the nominal stoichiometry. CZTS films also have good optoelectronic properties (a high absorption coefficient of  $\sim 10^4 \text{ cm}^{-1}$ ) and contain no toxic materials, making them desirable candidates for photovoltaic materials.

CZTS thin films have been prepared by several methods, such as sulfurization of sputtered [3–5] or evaporated [6] stacked films, the spray method [7,8], the sol-gel method [9], hydrazine deposition [10], electrode deposition [11] and co-evaporation [12]. Experimentally, it is found that CZTS and CZTSe thin films crystallize both in kesterite or stannite type structures [1–13], the first being the most common. CZTS thin films in the stannite type structure with a large absorption coefficient could be realized with a band gap of around 1.51 eV [13] when the ratios of the constituents in the CZTS thin films are close to stoichiometric. Currently, the conversion efficiency

of CZTS and CZTSe-based solar cells is around 7% and 10% respectively [10,14–17].

Although high, the efficiency is still well below the limit determined by the detailed balance between the solar cell and the sun modeled as a black body. By modifying some of the physical properties of this semiconductor, the efficiency could be increased. It is known that the insertion of intermediate states into the band gap of a semiconductor offers a potential route to high efficiency ( $> 60\%$ ) [18]. For example, the isoelectronic doping of II–VI compounds with oxygen has shown that oxygen gives rise to deep traps [19–23] at which carriers recombine radiatively [22–28], increasing the efficiency.

There are theoretical [29–31] and neutron scattering experimental [32,33] studies of CZTS currently focusing on the impact of structural modifications. Indeed, a large variety of isolated intrinsic point defects and complexes can be formed. However, there are few studies about the isolated substitutional impurities.

In order to further improve the conversion efficiency of CZTS based solar cells, it is important to investigate the effect of the insertion of intermediate states into the band gap. In this work, we report the electronic properties of O-doped CZTS using first-principles total-energy defect calculations. From the results, we estimate the potential of this compound as a thin-film based solar cell material for idealized conditions regarding sun light absorption and material quality.

## 2. Calculations

In this work, we investigate the structural and electronic properties using first-principles total-energy defect calculations within the density functional formalism. It is known that the band gaps obtained as differences between single-particle band structure energies within

the density functional formalism are underestimated with the generalized gradient approximation (GGA) and the local spin density approximation (LDA) because of correlation problems. Nevertheless, if total defect formation energies [34,35] are used instead of the single particle energies, correlation problems and systematic errors are decreased [36]. Therefore, in this work we use total defect formation energies.

For the incorporation of an O atom into a S location ( $O_S$  substitution), the donor and acceptor energies correspond to the  $O_S^{1+}/O_S^0$  and  $O_S^0/O_S^{1-}$  transformations respectively. The formation energies for these transformations are  $\Delta H_f(O_S^{\pm}) = E(O_S^{\pm}) - E_H - \mu_O + \mu_S \pm \mu_e$ , where  $E(O_S^{\pm})$  denotes the total incorporation energy,  $E_H$  is the total energy of the host,  $\mu_e$  is the Fermi energy, and  $\mu_O$  and  $\mu_S$  denote the O and S chemical potentials respectively. These chemical potentials represent the energies of the reservoirs with which atoms are being exchanged. The formation energy of negatively charged species (acceptors) decreases as  $\mu_e$  shifts from the valence band (VB) edge to the conduction band (CB) edge, while that of positively charged species (donors) decreases as  $\mu_e$  shifts from the CB edge to the VB edge. The turning points of the  $O_S^0/O_S^{1-}$  and  $O_S^{1+}/O_S^0$  transformations mark the transition energy levels:  $e_A = E(O_S^{1-}) - E(O_S)$  and  $e_D = E(O_S) - E(O_S^{1+})$ . Therefore, the  $\mu_e$  energy range in which the charge state  $O_S$  is stable is between  $e_D$  and  $e_A$ . The  $O_S^{1+}$  and  $O_S^{1-}$  charge states are stable when  $\mu_e$  is below  $e_D$  and above  $e_A$  respectively. For the host semiconductor, the acceptor and donor energies correspond to the CB and VB edge energies, i.e.  $e_C$  and  $e_V$ . The band gap is  $E_g = e_C - e_V = E(S_S^{1-}) - 2E_H + E(S_S^{1+})$ .

In order to obtain the total defect formation energies, the standard Kohn-Sham [37] equations are solved self-consistently [38] using a confined pseudoatomic orbital [39] basis set. For the exchange-correlation potential, we use the GGA of Perdew, Burke, and Ernzerhof [40,41], and the LDA with the Perdew-Zunger parameterization to the Ceperley-Alder numerical data [42]. The standard Troullier-Martins [43] pseudopotential is adopted and expressed in the Kleinman-Bylander [44,45] factorized form.

From the literature [1-12,32,33], CZTS crystallizes mainly in the kesterite type structure. Thus this is the structure analyzed in this work. The experimental [46] lattice parameters of the CZTS in the kesterite type structure are  $a = 5.427 \text{ \AA}$  and  $c/2a = 1.002$ . In order to study the CZTS:O alloys, we use a 64-atom supercell where one S atom is replaced by O. To reach the configuration of absolute energy minimum, the atomic positions around the defect are relaxed until the forces on the atoms fall below  $0.04 \text{ eV \AA}^{-1}$ . The results in this work refer to substituted lattice structures, in the sense that no isolated point defects and complexes nor combinations of them other than the specific substitution proposed have been allowed in the supercell. The substitutional impurities have no interaction with other intrinsic isolated point defects and complexes. Therefore, these results of substitutional impurities add to the results of isolated point defects and complexes.

### 3. Results and discussion

The CZTS band gap obtained using total energy defect calculations, i.e. the difference between the acceptor ( $e_C$ , CB edge) and donor ( $e_V$ , VB edge) energies, is 1.61 eV. This result compares well with experimental data in the literature, between 1.4 eV [1] and 1.6 eV [2], and with other theoretical data in the literature ( $\sim 1.5 \text{ eV}$  [47,48]). When S is substituted by O, the O is surrounded by one Zn, one Sn and two Cu atoms. The electronic structure of the O-doped CZTS is characterized by a sub-band in the band gap close to the CB with an acceptor character. Fig. 1 shows the band diagram with GGA and LDA. The sub-band is made up by the combination of the O-2p and Sn-5s orbitals. The difference between the acceptor energy and the CB edge is  $e_C - e_A = 0.53 \text{ eV}$ .

In this material the position of the sub-band depends strongly on the electronic density and, as a consequence, on the atomic positions.

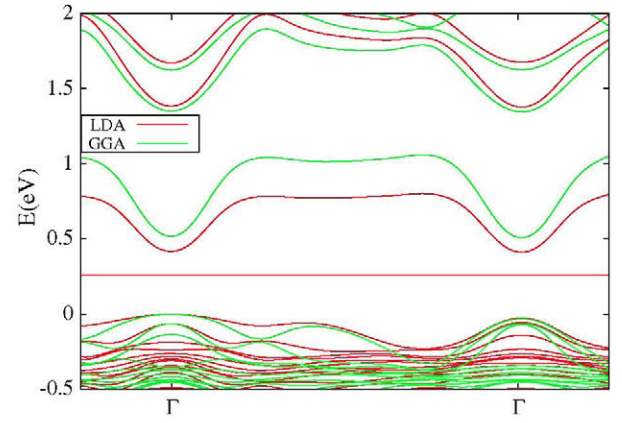


**Fig. 1.** Energy-band diagram of the CZTS:O with a 64-atom cell using GGA and LDA. The VB edge has been chosen as the energy origin.

The total defect formation energy, and therefore the ionization energies, also depends on the atomic positions. The donor energy of CZTS:O is almost always below the VB. In order to analyze the evolution of the acceptor energy with the environment of the O atom, we have considered the inward and outward displacement of the nearest neighbors of the O atom, i.e. breathing-modes (Fig. 2). The O atom is coordinated by two Cu atoms, one Sn atom, and one Zn atom in a first shell, and by 12 S atoms in a second shell. In this breathing-mode, the distances to the nearest neighbors are scaled with respect to the distances of the energy minima  $Q_0$ :  $Q = \alpha Q_0$  (inward relaxation for  $0 < \alpha < 1$ , and outward relaxation for  $\alpha > 1$ ). We have chosen this breathing mode because the force constants and the displacement

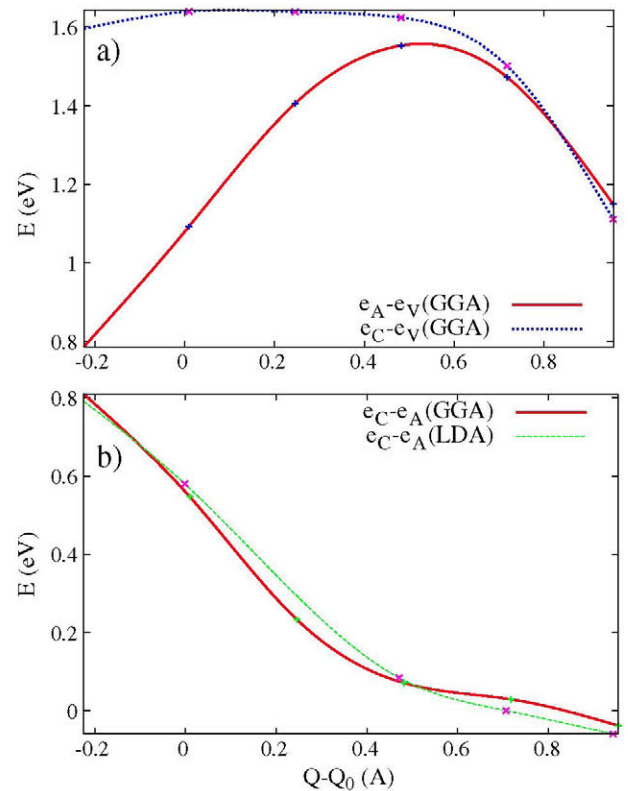


**Fig. 2.** (a) Acceptor ( $e_A$ ) and CB edge ( $e_C$ ) energies with respect to the VB edge ( $e_V$ ) energy as a function of  $Q - Q_0$  for CZTS:O with a 64-atom cell using GGA. (b) Energetic distance  $e_C - e_A$  versus  $Q - Q_0$  with LDA and GGA.  $Q$  is the generalized coordinate (distance O-Sn) and  $Q_0$  is its value for the energy minimum.



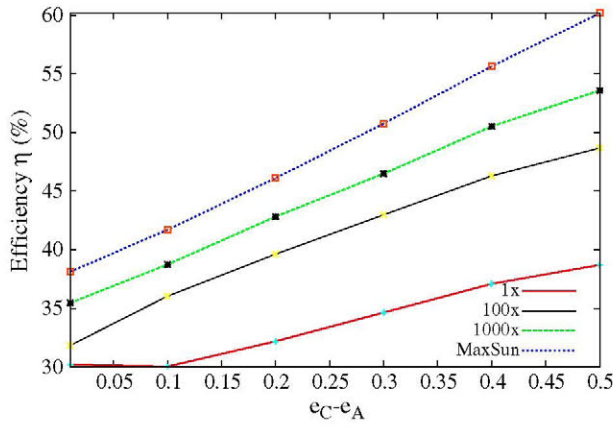


**Fig. 3.** Efficiency  $\eta$  (%) versus acceptor energy distance with respect to the CB edge ( $e_C - e_A$ ) for several sunlight concentrations.

of the equilibrium positions are larger than for other modes [49–51]. Therefore, in principle, their effect on the lattice dynamic will be larger.

For  $Q - Q_0 > 0$  (outward displacement) the band gap is reduced because the atoms of the first shell are closer to the atoms of the second shell. As a result, the interaction between the two shells increases and the band gap decreases. An inward relaxation ( $Q - Q_0 < 0$ ) decreases the acceptor ionization energy because of the increment in the interaction between the O atom with the four atoms in the first shell, in particular, with the Sn atom. As a global result, the acceptor ionization energy with respect to the CB edge decreases with increasing  $Q$  (Fig. 2). Fig. 2 also shows the strong dependence of the acceptor energy on the aforementioned atomic positions.

In order to determine if incorporation of O into CZTS leads to additional absorption of solar radiation with respect to the CZTS host, we estimate the theoretical maximum efficiency for solar energy conversion. Using the band gap and ionization energies from first-principles total defect formation energy calculations, we have obtained the efficiencies for several sunlight concentrations according to the model described in Ref. [18]. Calculations were carried out from 1 sun ( $1 \text{ kW/m}^2$ ) to maximum solar concentration (46050 suns). Fig. 3 shows the efficiency  $\eta$  against the acceptor energy distance with respect to the CB edge ( $e_C - e_A$ ) for several sunlight concentrations. From the figure, the efficiency increases with increasing  $e_C - e_A$  for all concentrations. For maximum solar concentration, the maximum efficiency obtained with O-doped CZTS is  $\sim 60\%$ . This maximum is larger than the efficiency of a single junction solar cell with equal solar concentration ( $< 40\%$ ). For concentrations larger than approximately 100 suns, the efficiency of the O-doped CZTS is larger than the maximum efficiency (for maximum solar concentration) of the host CZTS single junction solar cell.

#### 4. Conclusions

In summary, using total energy defect first-principles calculations with the density functional method, we have studied the ionization energies of O-doped CZTS. The electronic structure of O-doped CZTS is characterized by a sub-band in the band gap close to the CB. This deeper band is made up of a combination of the Sn-5s and O-2p orbitals. The analysis of the energetic distance from this level to the CB edge indicates an increment in energy when the distance from the O atom to its nearest neighbors is lower. Finally, the energetic position of the acceptor ionization level with respect to the CZTS band edges leads to an increment in solar energy conversion efficiency.

#### Acknowledgments

This work has been supported by the National Spanish projects Denquiband (PLE2009-0045), Bibiana (PIB2010US-00096) and Nanogefes (ENE2009-14481-C02-01), by the European Commission through the funding of the projects IBPOWER (Ref. N: Grant Agreement 211640) and NGCPV (283798), and by La Comunidad de Madrid through the funding of the project NUMANCIA-2 (Ref. N: S-2009/ENE-1477).

#### References

- [1] H. Katagiri, N. Ishigaki, T. Ishida, K. Saito, *Jpn. J. Appl. Phys.* 40 (2001) 500.
- [2] H. Katagiri, K. Saitoh, T. Washio, H. Shinohara, T. Kurumadani, S. Miyajima, *Sol. Energy Mater. Sol. Cells* 65 (2001) 141.
- [3] N. Momose, M. Than Htay, T. Yudasaka, S. Igarashi, T. Seki, S. Iwano, Y. Hashimoto, K. Ito, *Jpn. J. Appl. Phys.* 50 (2011) 01BG09.
- [4] H. Katagiri, *Thin Solid Films* 480 (2005) 426.
- [5] T. Tanaka, T. Nagatomo, D. Kawasaki, M. Nishio, Q. Guo, A. Wakahara, A. Yoshida, H. Ogawa, *J. Phys. Chem. Solids* 66 (2005) 1978.
- [6] A. Weber, H. Krauth, S. Perlt, B. Schubert, I. Kotschau, S. Schorr, H.W. Schock, *Thin Solid Films* 517 (2009) 2524.
- [7] N. Kamoun, H. Bouzouita, B. Rezig, *Thin Solid Films* 515 (2007) 5949.
- [8] H. Yoo, J. Kim, *Sol. Energy Mater. Sol. Cells* 95 (2011) 239.
- [9] K. Tanaka, M. Oonuki, N. Moritake, H. Uchiki, *Sol. Energy Mater. Sol. Cells* 93 (2009) 583.
- [10] T. Todorov, O. Gunawan, S.J. Chey, T. Goisard de Monsabert, A. Prabhakar, D.B. Mitzi, *Thin Solid Films* 519 (2011) 7378.
- [11] A. Ennaoui, M. Lux-Steiner, A. Weber, D. Abou-Ras, I. Kotschau, H.-W. Schock, R. Schurr, A. Holzing, S. Jost, R. Hock, T. Vo, J. Schulze, A. Kirbs, *Thin Solid Films* 517 (2009) 2511.
- [12] B.-A. Schubert, B. Marsen, S. Cinque, T. Unold, R. Klenk, S. Schorr, H.-W. Schock, *Prog. Photovoltaics Res. Appl.* 19 (2011) 93.
- [13] J. Zhang, L. Shao, *Sci. China, Ser. E* 52 (2009) 269.
- [14] H. Katagiri, K. Jimbo, S. Yamada, T. Kamimura, W.S. Maw, T. Fukano, T. Ito, T. Motohiro, *Appl. Phys. Express* 1 (2008) 041201.
- [15] T.K. Todorov, K.B. Reuter, D.B. Mitzi, *Adv. Mater.* 22 (2010) E156.
- [16] H. Katagiri, K. Jimbo, W.S. Maw, K. Oishi, M. Yamazaki, H. Araki, A. Takeuchi, *Thin Solid Films* 517 (2009) 2455.
- [17] J. Scragg, P. Dale, L. Peter, *Thin Solid Films* 517 (2009) 2481.
- [18] A. Luque, A. Martí, *Phys. Rev. Lett.* 78 (1997) 5014.
- [19] C. Tablero, *Comput. Mater. Sci.* 49 (2010) 368.
- [20] C. Tablero, *Appl. Phys. Lett.* 96 (2010) 121104.
- [21] B. Lee, L. Wang, *Appl. Phys. Lett.* 96 (2010) 071903.
- [22] Y. Burki, P. Sshwendimann, W. Czaja, H. Berger, *J. Phys. Condens. Matter* 5 (1993) 9235.
- [23] Y. Burki, P. Sshwendimann, W. Czaja, H. Berger, *Europhys. Lett.* 13 (1990) 555.
- [24] W. Wang, A.S. Lin, J.D. Phillips, W.K. Metzger, *Appl. Phys. Lett.* 95 (2009) 261107.
- [25] J.L. Merz, *Phys. Rev.* 176 (1968) 961.
- [26] W.K. Ge, S.B. Lam, I.K. Sou, J. Wang, Y. Wang, G.H. Li, H.X. Han, Z.P. Wang, *Phys. Rev. B* 55 (1997) 10035.
- [27] M.J. Seong, H. Alawadhi, I. Miotkowski, A.K. Ramdas, S. Miotkowska, *Phys. Rev. B* 60 (1999) R16275.
- [28] Y.M. Yu, S. Nam, K.-S. Lee, Y. Dae Choi, O. Byungsung, *J. Appl. Phys.* 90 (2001) 807.
- [29] S. Chen, J.-H. Yang, X.G. Gong, A. Walsh, S.-H. Wei, *Phys. Rev. B* 81 (2010) 245204.
- [30] S. Chen, X.G. Gong, A. Walsh, S.-H. Wei, *Appl. Phys. Lett.* 96 (2010) 021902.
- [31] A. Nagoya, R. Asahi, R. Wahl, G. Kresse, *Phys. Rev. B* 81 (2010) 113202.
- [32] S. Schorr, H.J. Hoebler, M. Tovar, *Eur. J. Mineral.* 19 (2007) 65.
- [33] S. Schorr, C. Stephan, R. Mainz, H. Rodriguez-Alvarez, M. Tovar, *Adv. Eng. Mater.* 13 (2011) 737.
- [34] C.G. Van de Walle, J. Neugebauer, *J. Appl. Phys.* 95 (2004) 3851.
- [35] J.E. Northrup, S.B. Zhang, *Phys. Rev. B* 47 (1993) 6791.
- [36] D.A. Drabold, S. Estreicher, *Theory of Defects in Semiconductors*, Springer, Berlin, Heidelberg, 2007.
- [37] W. Kohn, L.J. Sham, *Phys. Rev.* 140 (1965) A1133.
- [38] J.M. Soler, E. Artacho, J.D. Gale, A. García, J. Junquera, P. Ordejón, D. Sánchez-Portal, *J. Phys. Condens. Matter* 14 (2002) 2745 (and references therein).
- [39] O.F. Sankey, D.J. Niklewski, *Phys. Rev. B* 40 (1989) 3979.
- [40] J.P. Perdew, K. Burke, M. Ernzerhof, *Phys. Rev. Lett.* 77 (1996) 3865.
- [41] J.P. Perdew, K. Burke, M. Ernzerhof, *Phys. Rev. Lett.* 78 (1997) 1396.
- [42] D.M. Ceperley, B.J. Alder, *Phys. Rev. Lett.* 45 (1980) 566.
- [43] N. Troullier, J.L. Martins, *Phys. Rev. B* 43 (1991) 1993.
- [44] L. Kleinman, D.M. Bylander, *Phys. Rev. Lett.* 48 (1982) 1425.
- [45] D.M. Bylander, L. Kleinman, *Phys. Rev. B* 41 (1990) 907.
- [46] R.S. Hall, J.T. Szymanski, J.M. Stewart, *Can. Mineral.* 16 (1978) 131.
- [47] S. Chen, X.G. Gong, A. Walsh, S.-H. Wei, *Appl. Phys. Lett.* 94 (2009) 041903.
- [48] J. Paier, R. Asahi, A. Nagoya, G. Kresse, *Phys. Rev. B* 79 (2009) 115126.
- [49] D.V. Lang, C.H. Henry, *Phys. Rev. Lett.* 35 (1975) 1525.
- [50] K.V. Boer, *Survey of Semiconductor Physics*, John Wiley & Sons Inc., 2002.
- [51] C. Tablero, *J. Appl. Phys.* 108 (2010) 093114.